Time-reversal acoustics and ultrasound-assisted convection-enhanced drug delivery to the brain

William Olbricht[a)]
School of Chemical and Biomolecular Engineering and Department of Biomedical Engineering, Olin Hall, Cornell University, Ithaca, New York 14853

Manjari Sistla
Department of Biomedical Engineering, Weill Hall, Cornell University, Ithaca, New York 14853

Gaurav Ghandi
Artann Laboratories, Inc., 1459 Lower Ferry Road, Trenton, New Jersey 08618

George Lewis, Jr.[b)]
Department of Biomedical Engineering, Weill Hall, Cornell University, Ithaca, New York 14853

Armen Sarvazyan
Artann Laboratories, Inc., 1459 Lower Ferry Road, Trenton, New Jersey 08618

(Received 27 September 2012; revised 26 February 2013; accepted 4 March 2013)

Time-reversal acoustics is an effective way of focusing ultrasound deep inside heterogeneous media such as biological tissues. Convection-enhanced delivery is a method of delivering drugs into the brain by infusing them directly into the brain interstitium. These two technologies are combined in a focusing system that uses a "smart needle" to simultaneously infuse fluid into the brain and provide the necessary feedback for focusing ultrasound using time-reversal acoustics. The effects of time-reversal acoustics-focused ultrasound on the spatial distribution of infused low- and high-molecular weight tracer molecules are examined in live, anesthetized rats. Results show that exposing the rat brain to focused ultrasound significantly increases the penetration of infused compounds into the brain. The addition of stabilized microbubbles enhances the effect of ultrasound exposure.
 [http://dx.doi.org/10.1121/1.4812879]

PACS number(s): 43.80.Vj, 43.80.Gx [CCC] Pages: 1569–1575

I. INTRODUCTION

The use of therapeutic ultrasound in medical applications often requires focusing acoustic energy to a specific region of tissue that is the therapeutic target while minimizing exposure of healthy tissue surrounding the target. This can be a formidable challenge when the target is deep inside the body. Conventional methods of focusing that use concave transducers, lenses, and phased arrays work well in homogeneous media, but not in heterogeneous media, owing to wave front distortions caused by structural variations along the path of the acoustic beam. Multi-element arrays are more flexible in this respect. Because the array elements are fed from individual power amplifiers, phases and amplitudes can be varied at these elements. As a result, it is possible to control the phase relations over the entire array's aperture and form a wave front of the shape required to correct aberrations caused the medium's heterogeneity. However, the flexibility provided by phased arrays is achieved at the expense of their intricate design. They are often complicated, do not necessarily provide the required improvement, and can generate undesired grating lobes that focus acoustic energy outside the targeted region.

An alternative approach relies on principles of time-reversal acoustics (TRA) to focus ultrasound in highly heterogeneous and scattering media. TRA focusing is based on the reversibility in time of acoustic wave propagation. As a result of this reversibility, the time-reversed version of an incident acoustic signal focuses automatically on the source of the original signal.[1,2] TRA-based ultrasound focusing systems have been developed for delivering ultrasound to specified locations in heterogeneous media in a variety of physical and biological applications.[2–5] The goal of this paper is to demonstrate the benefits of TRA-based focusing in a medical application where previous studies have shown that ultrasound has the potential to significantly improve therapy.

Convection-enhanced delivery (CED) is a promising method of drug delivery to the brain for the treatment of several neurological disorders, including glioblastoma multiforme, a high-grade malignancy that presents an especially poor prognosis for patients.[6] CED circumvents the blood-brain barrier, which blocks the systemic delivery of many therapeutics, by infusing compounds through a needle inserted into the brain through a small hole in the skull. The infused liquid containing therapeutic compounds flows radially outward from the needle tip into surrounding brain tissue. Convection is the dominant interstitial transport mechanism near the needle tip. However, the convective velocity of the infusate in the interstitium decreases with

[a)]Author to whom correspondence should be addressed. Electronic mail: wlo1@cornell.edu
[b)]Current address: ZetrOZ, Inc., 56 Quarry Road, Trumbull, CT. 06611.

distance from the needle so that sufficiently far from the needle, both convection and diffusion influence mass transfer of compounds in the infusate.

CED has been used to infuse a variety of compounds into animal and human subjects, including low molecular weight molecules,[7,8] proteins,[9,10] viral vectors,[8,11,12] nanoparticles,[13,14] and liposomes.[15,16] Low molecular weight molecules move readily through the interstitium, but proteins and other high-molecular weight compounds, including some of the most promising drugs to treat neurological disorders, are strongly hindered during their motion through the brain interstitium, which limits the penetration of drugs into the brain during CED.

The results of CED therapy in preclinical and clinical studies have been highly variable. Promising drugs with established efficacy in preliminary studies have failed to produce consistently significant therapeutic benefits in clinical trials. The consensus among many practitioners is that inadequate distribution of infused drugs into the brain parenchyma is responsible for the disappointing results.[17] Indeed, results of numerous animal experiments and clinical trials suggest that the important challenges facing CED are to improve penetration of the infusate into the tissue and to control the spatial and temporal distribution of the infused drug to optimize its therapeutic potential.

Ultrasound is known to improve mass transfer in a variety of situations including some important medical applications. In many such instances, acoustic cavitation and resulting microstreaming[18,19] are the underlying mechanisms of ultrasound-enhanced drug delivery that lead to enhanced mass transfer. Measurements of tracers in brain slices *ex vivo* suggest that ultrasound enhances both diffusion and convection through neural tissue.[20] Experiments with live, anesthetized rodents showed that exposure of the brain to unfocused ultrasound increased the extent of penetration of a low-molecular weight tracer by about a factor of five.[21] Indeed, infused dye penetrated throughout most of the hemisphere of the rodent brain. In an experiment involving a larger animal, unfocused ultrasound increased the extent of distribution of labeled liposomes during CED infusion into the brain of a non-human primate.[22] In these experiments, a relatively large volume of tissue, i.e., the entire hemisphere of the brain, was exposed to unfocused ultrasound. However, it may be possible to enhance mass transfer of infused compounds during CED by selectively exposing a much smaller portion of the brain to focused ultrasound using the TRA method.

One way to focus acoustic energy by the TRA method is to place a beacon in the medium that provides an initial signal from the target region. A hydrophone placed at the chosen target is the most common beacon in TRA systems described in the literature. Highly reflective targets that provide an acoustical feedback signal could also serve as beacons for TRA focusing of the acoustic beam. In any case, the requirement of having a beacon placed at the target region often limits applications of TRA focusing of ultrasound, especially in medical applications. In this paper, we solve the "beacon problem" by infusing fluid into the brain using a proprietary "smart needle" developed at Artann Laboratories. To accurately focus ultrasound precisely at the point where fluid enters the tissue, the tip of the needle is equipped with a miniature piezotransducer that provides the required feedback signal to establish the TRA relationship between the transmitter and the target site in the brain. Thus the smart needle simultaneously delivers fluid to tissue and provides the signal that enables TRA focusing at the delivery site.

We have conducted a series of experiments using TRA focusing with the smart needle in brain-mimicking materials and in live, anesthetized rodents. The goals are to demonstrate that acoustic energy can be focused using TRA methods and to determine whether TRA-focused ultrasound increases the local rate of mass transfer in the region of focused ultrasound. This is the necessary first step in the design of an ultrasound focusing system to control the spatial distribution of infused compounds in CED therapy.

II. METHODS

A. Time-reversal acoustics and the smart needle

The TRA system (Artann Laboratories, Trenton, NJ) comprises an electronics unit, software, and a set of reverberators/transmitters to deliver ultrasound into the rodent brain from outside the skull. Although an enclosure such as the rodent skull could act as a reverberator for TRA focusing, it would be difficult to attach a sufficient number of piezoceramic disks directly onto the rodent skull owing to its small size. Therefore the TRA system uses an aluminum external reverberator with 18 piezoelectric crystals mounted at random positions and orientations inside an enclosure that tapers to a cone to match the size of the rodent skull. A waveform generator provides an initial excitation signal with a predefined waveform that is applied to each of the reverberator's channels.

The smart needle is a custom designed infusion catheter (Transducer Engineering, Inc., Waltham, MA) that contains a small hydrophone. The device consists of a 30-gauge stainless steel needle that is equipped with a longitudinal resonating piezotransducer with a center frequency of 0.5 MHz. The transducer is situated near the distal end of the needle and equipped with a wire that conducts the recorded signal to electrical connections in an aluminum guide tube that holds the needle. The smart needle hydrophone was calibrated with a low-frequency hydrophone (ONDA, Inc., Sunnyvale, CA) hydrophone in a 1-l water beaker.

During CED infusions, the smart needle records the acoustic signal at the site where fluid leaves the needle and enters the brain. The recorded signal is time-reversed, amplified, synchronized, and applied simultaneously to all of the transmitters. The modified signal focuses accurately at the target, which is a known volume of tissue surrounding the needle tip.

B. Infusions into brain-mimicking gels

To minimize the number of animals used in experiments, ultrasound parameters for the animal experiments

were chosen based on results of preliminary experiments conducted with brain mimicking phantoms.

A small, clear plastic vial was filled with 0.6% agarose gel, which is often used as a brain mimic for CED experiments.[23] In some experiments, cotton fibers (1 wt. %) were added to the gel to examine effects of local heterogeneities on mass transfer. The infusate was water that contained a trace amount of red food coloring. To examine effects of microbubbles on mass transfer, Targestar-P (TS 108) stabilized microbubbles were added to the fluid. The number density of microbubbles in the infusate was 5×10^5 microbubbles/μl.

The ultrasound frequency was 750 kHz. The time-averaged intensity was about 20 mW/cm^2 and peak-to-peak acoustic pressure was maintained in the range 150–250 kPa.

The smart needle was held in a three-dimensional positioning system and then lowered into the gel as shown in Fig. 1. Once the smart needle was in place, the TRA system was activated, and 10 μl of water containing red food coloring was infused through the needle into the gel in a short time (about 1 min). Ultrasound exposure continued for 30 min following the infusion of the dye into the gel. Control experiments were done in the identical way except that the TRA system was not activated.

At the end of the ultrasound exposure, the gel was removed from the plastic vial and cut in half in a plane that contained the needle insertion point. Each half of the gel was photographed, cropped to uniform dimensions in Adobe PHOTOSHOP (Adobe Systems, Inc., San Jose, CA) and analyzed with MATLAB (The Mathworks, Inc., Natick, MA) software. The colored part of the image was separated from background, the boundary of the dye distribution was circumscribed, and the diameter of the colored area, which was close to circular in every case, was measured. From that measurement, the volume of distribution of dye was calculated for a spherical distribution.

C. Infusions into anesthetized rodents

The Institutional Animal Care and Use Committee at Cornell University approved all animal protocols. Male albino Sprague–Dawley rats (375–450 g, Charles Rivers Associates, USA) were used for the experiments. Each rat was anesthetized with a mixture of oxygen (0.8 l/min at 1.0 bar, 21 °C) and 1.5%–2.0% vaporized isoflurane (Aerrane, Baxter Healthcare, Deerfield, IL) using an anesthesia vaporizer. A heating pad maintained body temperature at 37 °C.

The rodent experiment is shown schematically in Fig. 2. The anesthetized animal was secured in a stereotaxic frame, and a 2-cm incision was made in the skin along the dorsal midline of the skull. A 1-mm burr hole was then drilled with a dental drill at +0 mm anterior and +3 mm lateral to Bregma. The reverberator was then positioned on the right side of the skull and coupled to the skull with ultrasound gel.

The smart needle was guided by a micromanipulator and lowered into the brain at a depth of 5.5 mm. After waiting 2 min for the brain to equilibrate, focusing measurements were made along the insertion path. Good acoustic coupling between the reverberator and skull gave a signal-to-noise ratio of about 7 dB and a focal volume that was about 2 mm in diameter.

Based on the preliminary experiments in gels and previous studies, ultrasound parameters were set to 1-MHz frequency, 8-μs pulse duration, burst mode with eight pulse repetitions, a maximum acoustic pressure between 100 and 200 kPa, an ultrasonic intensity between 10 and 40 mW/cm^2, and 0.2-MHz bandwidth.

Two infusates were used in separate experiments: A 0.25% wt./vol. solution of Evan's blue dye (EBD) in phosphate buffered saline and a 0.25% wt./vol. solution of albumin-conjugated EBD in phosphate buffered saline. EBD and albumin-conjugated EBD are representative of low- and high-molecular weight therapeutics, respectively. Each solution was passed through a 0.22-μm syringe filter before it was loaded into the smart needle. To show the effect of microbubbles on the extent of infusate penetration, Targestar microbubbles with a number density of 1×10^6 microbubbles/μl were mixed into EBD in 1:1 ratio. Each experimental group (EBD vs albumin-conjugated EBD and no microbubbles vs microbubbles contained four subjects, $n = 4$).

The infusate tracer solution was loaded into an infusion pump apparatus (Bee Stinger 1000-μl gas tight syringe and pump by BASi Preclinical Services, IN, USA), which was

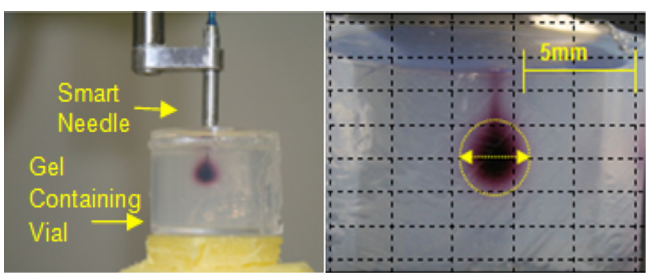

FIG. 1. (Color online) Infusion of dye into an agarose gel. Left: The smart needle containing the TRA hydrophone is inserted into 0.6% agarose gel contained in a transparent vial. Right: The infused dye at the completion of the experiment. The infusion cloud is nearly spherical with diffuse edges. The yellow circle shows the boundary of the infusion cloud.

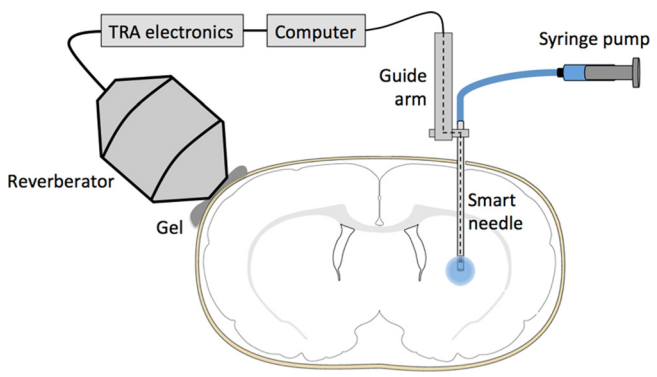

FIG. 2. (Color online) A schematic of the rodent experiment. The smart needle is attached to a guide arm that allows precise placement of the needle. A syringe pump infuses tracer through the smart needle. A hydrophone is freely suspended at the distal end of the smart needle to measure the acoustic signal there. A wire from the hydrophone is threaded up the needle and guide arm and connected to a computer that records the acoustic signal. The resulting signal is time reversed, and the time reversed signal is sent to an external reverberator coupled with gel to the outside of the rodent skull.

connected to the smart needle with PVC microtubing. The infusion pump delivered 0.2 μl/min continuously. The infusate was delivered into the brain at this rate for 2.5 min. Ultrasound exposure with TRA focusing was initiated at the start of the experiment and was maintained for a total of 30 min. Controls were also run with the identical procedure except the ultrasound was not activated.

Immediately following the experiment, the animal was euthanized by pentobarbital injection. The brain was removed and stored in 4% paraformaldehyde for 24 h, in a 30% aqueous sucrose solution for 48 h, and then in a 60% aqueous sucrose solution for 48 h.

The brain was then frozen on dry ice in optimal cutting temperature compound (Sakura Tissue Tek, Inc., Torrance, CA) and subsequently sliced in 50-μm slices on a microtome (Micom HM 550, ThermoFisher Scientific, Inc., Waltham, MA). Images of the frozen sections were made with a CCD camera (Canon Power Shot G10, Canon, Inc., Lake Success, NY).

Digital image files were cropped to include the rodent brain's caudate putamen with a locked aspect ratio using Adobe PHOTOSHOP. The modified images were processed through a MATLAB script to calculate the distribution volume of infused dye for each experiment. From the measured distribution volume V_d and the known volume of fluid infused V_i, the ratio V_d/V_i was calculated. This ratio is typically larger than unity because infused fluid flows only through the interstitial space between cells. The porosity of brain tissue is about 0.2, which means that the ratio V_d/V_i for a molecule that moves exactly with the infused fluid should be about 1/0.2 or 5.

To assay for neural damage as a result of the experiment, 4-μm thick brain slices were prepared and placed on a microscope slide. Slices were obtained near the infusion site and from distant locations where no dye was present at the end of the experiment for experimental runs with and without ultrasound exposure. The slices were analyzed by hematoxylin and eosin (H&E) staining using standard paraffin embedding and sectional procedures. A pathologist at the Cornell College of Veterinary Medicine, who was not otherwise involved in the experiments, examined the slices, which were not identified, and scored results.

III. RESULTS

A. TRA-focused ultrasound enhancement in brain-mimicking gels

Figure 1 shows a typical infusion into agarose gel at the end of the experiment after the smart needle was removed. The distribution of the infusate was close to spherical with a diffuse boundary.

The distribution volume is defined as the volume of the gel that was colored by the infused dye at the end of the experiment. To determine the effect of TRA-focused ultrasound on the CED infusion, the distribution volume with ultrasound was compared with the distribution volume without ultrasound (the control). For the case of infusion into pure gels, the distribution volume with ultrasound was larger than the distribution volume for the control by a factor of 7.2 ± 0.4. For the case of infusion into gels loaded with cotton fibers, the distribution volume with ultrasound increased by a factor of 8.2 ± 0.4.

B. TRA-focused ultrasound enhancement in anesthetized rodents

Experiments were carried out in anesthetized rodents to examine effects of TRA-focused ultrasound on the distribution of infused tracers. The infusion rate of 0.2 μl/min and infusion time of 2 min were chosen so that a small volume of tracer was introduced into the caudate, which is gray matter. This allowed measurements of the spread of the infusate and the enhancement in distribution volume owing to TRA-focused ultrasound without the infusate extending beyond the caudate into surrounding heterogeneous tissue structures.

Figure 3 is a composite of brain slices that covers the various experiments carried out in this study. In each case, the slice shown in the figure is the slice that contained the

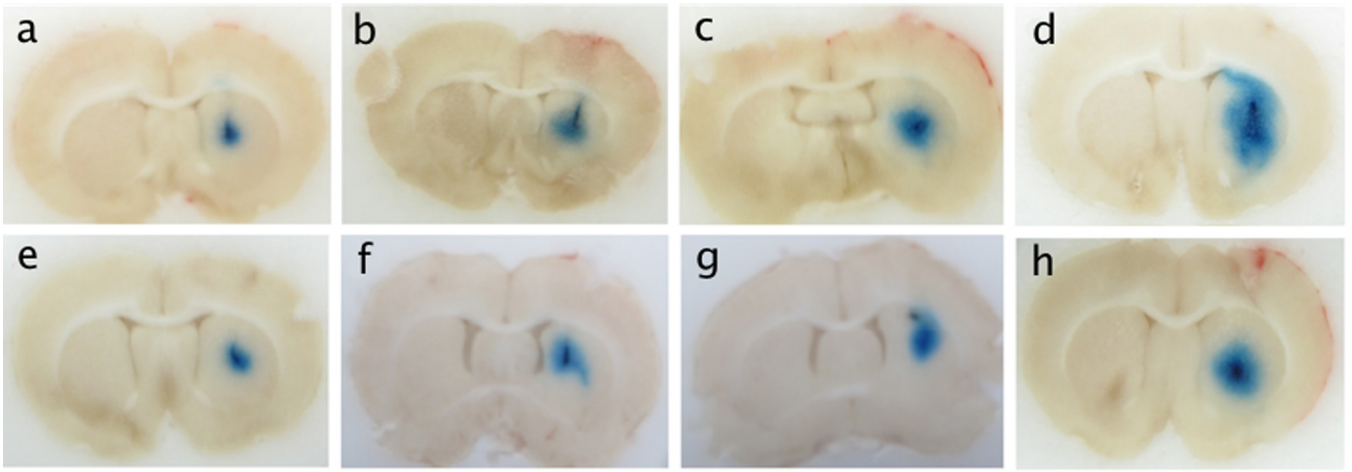

FIG. 3. (Color online) Typical coronal slices of rat brains illustrating the infusion of EBD and albumin-conjugated EBD. (a) EBD, no ultrasound, no microbubbles; (b) EBD, ultrasound, no microbubbles; (c) EBD, no ultrasound, microbubbles; (d) EBD, ultrasound, microbubbles; (e) albumin-conjugated EBD, no ultrasound, no microbubbles; (f) albumin-conjugated EBD, ultrasound, no microbubbles; (g) albumin-conjugated EBD, no ultrasound, microbubbles; (h) albumin-conjugated EBD, ultrasound, microbubbles.

smart needle. The smaller areas of dye coverage occurred in Figs. 3(a) and 3(e), which pertain to infusions of EBD [Fig. 3(a)] and albumin-conjugated EBD [Fig. 3(e)] without microbubbles and without ultrasound. When TRA-focused ultrasound was applied, there was a measureable enhancement of the distribution as shown in Fig. 3(b) for EBD and Fig. 3(f) for albumin-conjugated EBD. The inclusion of stabilized microbubbles in the infusate caused an increase in the distribution volume as shown in Fig. 3(c) for EBD and Fig. 3(g) for albumin-conjugated EBD. However, the greatest enhancement of dye coverage occurred when the infusate contained stabilized microbubbles and TRA-focused ultrasound was applied, as seen in Fig. 3(d) for EBD and Fig. 3(h) for albumin-conjugated EBD.

Results for all subjects are compiled in Fig. 4 that confirm the qualitative results shown in Fig. 3. Exposure of tissue to TRA-focused ultrasound influenced the magnitude of the distribution volume both with and without microbubbles in the infusate. In the absence of microbubbles, the distribution volume of EBD increased by 75%, and the distribution volume of albumin-conjugated EBD increased by about 91%. Results for the cases with microbubbles in the infusate are qualitatively similar. In these cases, comparisons between distribution volumes with and without ultrasound showed an increase due to TRA-focused ultrasound of 120% for EBD with microbubbles and 107% for albumin-conjugated EBD with microbubbles.

The figure also shows that in every case, the distribution volume for albumin-conjugated EBD was smaller than the distribution volume for EBD. This is expected based on the difference in molecular weights of the two molecules. The albumin-conjugated dye is about 100 times larger than the dye alone, which increases hindrance of the conjugated dye as it moves through the interstitium by convection or diffusion. Exposing the tissue to TRA-focused ultrasound did not affect this molecular size-dependence on the distribution volume.

It is interesting to note that even in the absence of ultrasound, distribution volumes were larger when the infusate was seeded with microbubbles. This may be due to local edema near the infusion site that may be exacerbated by the microbubbles, which are used mostly as a contrast agent in blood not in tissue interstitium. Another possibility is that the microbubbles accumulated at the needle tip producing a region of low porosity there; this would cause the infused liquid to move farther from the needle tip.

To obtain more detailed information about the distribution volumes for the various cases, the area of dye in each slice was plotted as a function of distance in the anterior-posterior direction between the slice of interest and the slice that contained the smart needle. This is shown in Fig. 5 for EBD and in Fig. 6 for albumin-conjugated EBD. Each point is an average over four subjects in each group. The slices near the smart needle (zero on the x axis) showed greater penetration of dye than the more distant slices far from the needle in both directions. Penetration of dye in each slice was greater for the EBD than for the albumin-conjugated EBD. Furthermore, the EBD penetrated further from the smart needle than did the albumin-conjugated EBD. An analysis of the data showed that the points close to the smart needle were consistent with a spherical infusion of dye surrounding the smart needle. However, for points more distant from the smart needle, penetration of the dye was favored in the anterior-posterior direction, resulting in a three-dimensional distribution volume that was closer to an ellipsoid than a sphere with the major axis in the anterior-posterior direction.

Histology showed minor differences in the sample tissue slices from the four experimental groups. Small hemorrhages around the needle track and some edema around the insertion point, both common in CED experiments, were visible. Small hemorrhages were also visible on the cortical surface; this is likely due to the weight of the reverberator. The groups with microbubbles present showed slightly more hemorrhages and edema around the needle insertion.

IV. DISCUSSION

The total volume of dye infused in this experiment was 0.5 μl. The porosity of brain tissue is estimated to be about 0.2. Thus if the infused dye formed a sphere around the tip of the smart needle, the radius of the sphere at the end of the infusion would be about 0.8 mm, ignoring effects of dye diffusion. Previous measurements of the acoustic field

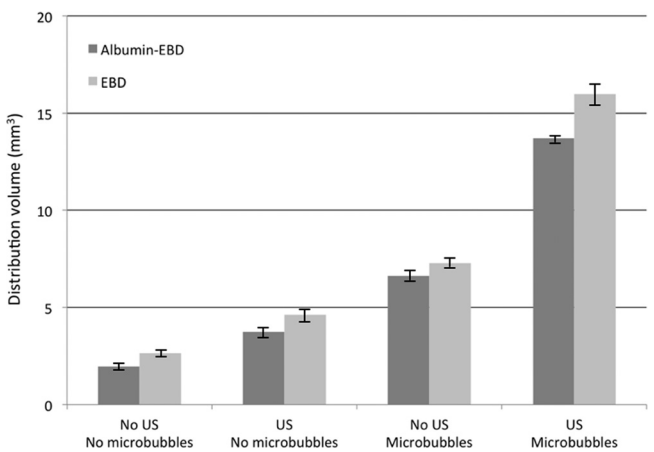

FIG. 4. Average measured distribution volumes of EBD and albumin-conjugated EBD ($n = 4$). The standard error for each group is shown.

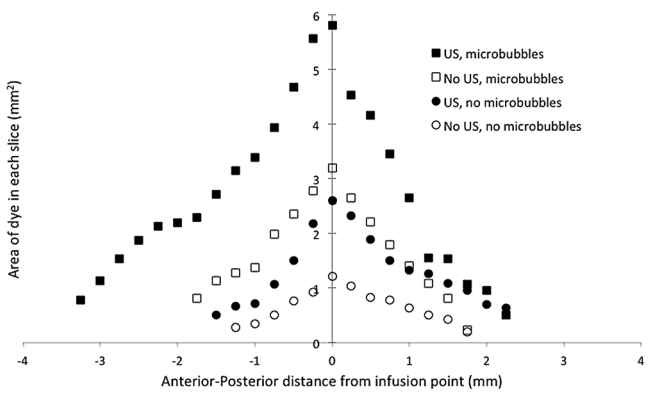

FIG. 5. The area that EBD covered in each coronal slice as a function of distance from the infusion point in the anterior-posterior direction. The value of "0" corresponds to the location of the smart needle. Each value is an average over subjects in each group ($n = 4$).

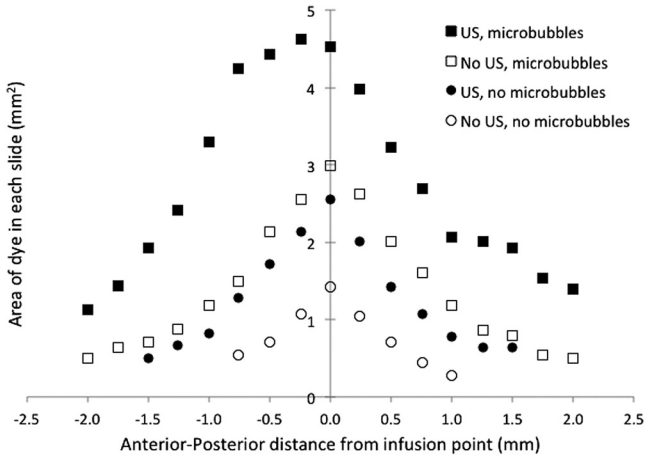

FIG. 6. The area that albumin-conjugated EBD covered in each coronal slice as a function of distance from the infusion point in the anterior-posterior direction. The value of "0" corresponds to the location of the smart needle. Each value is an average over subjects in each group ($n = 4$).

produced by the smart needle in brain tissue showed that the radius of the TRA focal volume is about 1 mm. Thus the infused material in these experiments should reside inside the TRA focal volume at least for short times.

Small molecules like EBD should move with the fluid by convection without hindrance from the surrounding interstitium. Because the porosity is about 0.2, the ratio V_d/V_i, where V_d is the distribution volume and V_i is the infusion volume, should be about 5 if the dye is confined to the extracellular space. The measured value of V_d/V_i for EBD without microbubbles and without ultrasound was 5.2 ± 0.31, which is close to the expected value for a small molecule. The corresponding ratio for albumin-conjugated EBD without microbubbles was 3.9 ± 0.34. Thus the motion of albumin-conjugated EBD lagged the motion of the liquid during the infusion, which is expected based on hindrance of the larger albumin molecule. The ratio V_d/V_i was much larger when the tissue was exposed to TRA-focused ultrasound, attaining values of 32.0 ± 1.1 for EBD with microbubbles and 27.4 ± 0.4 for albumin-conjugated EBD with microbubbles.

These results show that when a volume of tissue surrounding the smart needle was exposed to TRA-focused ultrasound, mass transfer was enhanced even at distances outside the TRA focal volume. The enhancement was greater when the infusate contained stabilized microbubbles. The tracer concentration is a continuous function throughout the tissue; this implies that changes in concentration inside the focal volume can affect concentration outside the tissue volume. For example, enhanced convection of the dye throughout the TRA focal volume could increase the magnitude of the concentration gradient at the boundary of the focal volume, which would enhance diffusion *outside* the focal volume.

Improving the outcome of CED therapy involves not only increasing the extent of penetration of infusate into surrounding tissue but also controlling the direction of penetration so that therapeutics are guided toward diseased tissue and away from healthy tissue and structures such as ventricles or large white matter tracts that can divert infusate from the intended target. TRA-focused ultrasound may provide the means to accomplish this goal. Focal volumes of arbitrary shape can be constructed by superimposing time-reversed impulse responses at several points. This can be achieved by using several smart needles simultaneously in a target region. Recording a set of impulse responses along the insertion path of the catheters provides a library of signals, enabling creation of the focal spot of desired 3D shape. The feasibility of forming composite focal patterns with complex shapes has been demonstrated.[24,25] Coupling this capability with CED delivery is currently underway in our laboratories.

V. CONCLUSIONS

The use of a smart needle to infuse fluid in CED coupled with TRA-focused ultrasound in the tissue surrounding the tip of the needle improved the volume of distribution of EBD and albumin-conjugated CED in experiments in live, anesthetized rodents. The enhancement in tracer penetration was greater when the infusate was seeded with stabilized microbubbles. Detailed analysis of brain slices post mortem revealed that the shape of the distribution volume is close to spherical in the tissue immediately adjacent to the needle tip, but the shape is more elongated in the anterior-posterior direction further away from the needle tip. The effect of the TRA-focused ultrasound on tracer penetration propagated beyond the focal volume of the ultrasound; this may be of significant benefit to CED where the goal is to promote penetration of therapeutic molecules dissolved in the infusate.

ACKNOWLEDGMENTS

This work was supported in part by National Institutes of Health Grant Nos. 1R21CA164935 and 1R43NS065524. The authors thank Dr. T. L. Southard of the Cornell College of Veterinary Medicine for evaluating tissues samples provided by the authors. The authors also thank Sabrina Guarino for her assistance in preliminary experiments.

[1]M. Fink, "Time reversed acoustics," Sci. Am. **281**, 91–97 (1999).
[2]M. Fink, G. Montaldo, and M. Tanter, "Time-reversal acoustics in biomedical engineering," Annu. Rev. Biomed. Eng. **5**, 465–497 (2003).
[3]M. Pernot, J. F. Aubry, M. Tanter, A. L. Boch, F. Marquet, M. Kujas, D. Seilhean, and M. Fink, "In vivo transcranial brain surgery with an ultrasonic time reversal mirror," J. Neurosurg. **106**, 1061–1066 (2007).
[4]A. P. Sarvazyan, L. Fillinger, and L. R. Gavrilov, "A comparative study of systems used for dynamic focusing of ultrasound," Acoust. Phys. **55**, 630–637 (2009).
[5]Y. D. Sinelnikov, A. M. Sutin, A. Y. Vedernikov, and A. P. Sarvazyan, "Time reversal acoustic focusing with a catheter balloon," Ultrasound Med. Biol. **36**, 86–94 (2010).
[6]R. H. Bobo, D. W. Laske, A. Akbasa, P. F. Morrison, R. L. Dedrick, and E. H. Oldfield, "Convection-enhanced delivery of macromolecules in the brain," Proc. Natl. Acad. Sci. **91**, 2076–2080 (1994).
[7]J. D. Heiss, S. Walbridge, A. R. Asthagiri, and R. R. Lonser, "Image-guided convection-enhanced delivery of muscimol to the primate brain," J. Neurosurg. **112**, 790–795 (2010).
[8]S. Oh, R. Odland, S. R. Wilson, K. M. Kroeger, C. Liu, P. R. Lowenstein, M. G. Castro, W. A. Hall, and J. R. Ohlfest, "Improved distribution of small molecules and viral vectors in the murine brain using a hollow fiber catheter," J. Neurosurg. **107**, 568–577 (2007).
[9]G. W. Astary, S. Kantorovich, P. R. Carney, T. H. Mareci, and M. Sarntinoranont, "Regional convection-enhanced delivery of gadolinium-labeled albumin in the rat hippocampus in vivo," J. Neurosci. Methods **187**, 129–137 (2010).

[10]D. Yin, J. Forsayeth, and K. S. Bankiewicz, "Optimized cannula design and placement for convection-enhanced delivery in rat striatum," J. Neurosci. Methods **187**, 46–51 (2010).
[11]E. White, A. Bienemann, L. Megraw, C. Bunnun, and S. Gill, "Evaluation and optimization of the administration of a selectively replicating herpes simplex viral vector to the brain by convection-enhanced delivery," Cancer Gene Ther. **18**, 358–369 (2011).
[12]M. S. Fiandaca, V. Varenika, J. Eberling, T. McKnight, J. Bringas, P. Pivirotto, J. Beyer, P. Hadaczek, W. Bowers, J. Park, H. Federoff, J. Forsayeth, and K. S. Bankiewicz, "Real-time MR imaging of adeno-associated viral vector delivery to the primate brain," Neuroimage **47** Suppl. 2, T27–35 (2009).
[13]K. B. Neeves, A. J. Sawyer, C. P. Foley, W. M. Saltzman, and W. L. Olbricht, "Dilation and degradation of the brain extracellular matrix enhances penetration of infused polymer nanoparticles," Brain Res. **1180**, 121–132 (2007).
[14]M. Y. Chen, A. Hoffer, P. F. Morrison, J. F. Hamilton, J. Hughes, K. S. Schlageter, J. Lee, B. R. Kelly, and E. H. Oldfield, "Surface properties, more than size, limiting convective distribution of virus-sized particles and viruses in the central nervous system," J. Neurosurg. **103**, 311–319 (2005).
[15]A. Y. Grahn, K. S. Bankiewicz, M. Dugich-Djordjevic, J. R. Bringas, P. Hadaczek, G. A. Johnson, S. Eastman, and M. Luz, "Non-PEGylated liposomes for convection-enhanced delivery of topotecan and gadodiamide in malignant glioma: Initial experience," J. Neuro-Oncol. **95**, 185–197 (2009).
[16]M. T. Krauze, S. R. Vandenberg, Y. Yamashita, R. Saito, J. Forsayeth, C. Noble, J. Park, and K. S. Bankiewicz, "Safety of real-time convection-enhanced delivery of liposomes to primate brain: A long-term retrospective," Exp. Neurol. **210**, 638–644 (2008).
[17]J. H. Sampson, G. Archer, C. Pedain, E. Wembacher-Schroder, M. Westphal, S. Kunwar, M. A. Vogelbaum, A. Coan, J. E. Herndon, R. Raghavan, M. L. Brady, D. A. Reardon, A. H. Friedman, H. S. Friedman, M. I. Rodriguez-Ponce, S. M. Chang, S. Mittermeyer, D. Croteau, and R. K. Puri, "Poor drug distribution as a possible explanation for the results of the PRECISE trial," J. Neurosurg. **113**, 301–309 (2010).
[18]W. G. Pitt, G. A. Husseini, and B. J. Staples, "Ultrasonic drug delivery—a general review," Expert Opin. Drug Deliv. **1**, 37–56 (2004).
[19]V. G. Zarnitsyn, P. P. Kamaev, and M. R. Prausnitz, "Ultrasound-enhanced chemotherapy and gene delivery for glioma cells," Technol. Cancer Res. Treat. **6**, 433–442 (2007).
[20]G. K. Lewis, Jr., W. L. Olbricht, and G. K. Lewis, "Acoustically enhanced Evans blue dye perfusion in neurological tissues," J. Acoust. Soc. Am. **2**, 20001–200017 (2008).
[21]G. K. Lewis, Jr., Z. Schultz, S. Pannullo, and W. L. Olbricht, "Ultrasound assisted convection enhanced drug delivery to the brain in vivo with novel transducer cannula assembly," J. Neurosurg. **117**, 1128–1140 (2012).
[22]Y. Liu, S. Paliwal, K. S. Bankiewicz, J. R. Bringas, G. Heart, S. Mitragotri, and M. R. Prausnitz, "Ultrasound-enhanced drug transport and distribution in the brain," AAPS PharmSciTech **11**, 1005–1017 (2010).
[23]Z.-J. Chen, G. T. Gillies, W. C. Broaddus, S. S. Prabhu, H. Fillmore, R. M. Mitchell, F. D. Corwin, and P. P. Fatouros, "A realistic brain tissue phantom for intraparenchymal infusion studies," J. Neurosurg. **101**, 314–322 (2004).
[24]B. K. Choi, A. Sutin, and A. Sarvazyan, "Formation of desired waveform and focus structure by time reversal acoustic focusing system," in *Proceedings of the 2006 IEEE International Ultrasonics Symposium*, Vancouver, Canada (2006), pp. 2177–2181.
[25]A. Sarvazyan, L. Fillinger, and L. Gavrilov, "Time-reversal acoustic focusing system as a virtual phased array," IEEE Trans. Ultrason. Ferroelect. Freq. Control **57**, 812–817 (2010).